Int. J. Heat Mass Transfer. Vol. 32, No. 4, pp. 639–654, 1989
Printed in Great Britain

0017–9310/89 $3.00 + 0.00

A comprehensive analysis of direct contact condensation of saturated steam on subcooled liquid jets

G. P. CELATA, M. CUMO, G. E. FARELLO and G. FOCARDI
ENEA CASACCIA Heat Transfer Laboratory, Via Anguillarese, 301, 00060 Roma, Italy

(*Received* 3 *March* 1988 *and in final form* 4 *July* 1988)

Abstract—An experiment on direct contact condensation of saturated steam on subcooled liquid jets is performed together with a theoretical analysis of the experimental data. Correlations available in the literature are generally unable to predict both the local conditions of the liquid jet and the total heat transfer. From the analysis of the local and global fluid-dynamics effects, a calculation method is proposed based on an equivalent thermal conductivity of the liquid jet. Comparison with the experimental data looks acceptable and well within the experimental accuracy.

1. INTRODUCTION

DIRECT contact heat transfer condensation phenomenon is of great interest both in the LWR nuclear industry (normal working of the pressurizer, pressure suppression in safety analysis, etc. [1]) and in the conventional industry (mixing-type heat exchangers, thermal degasifiers, sea-water desalting by multiple distillation, etc. [2]).

This paper deals with the results of an investigation of vapour condensation on a liquid jet.

The difference between most of the experiments available in the literature [3, 4] and those reported here is that the temperature of the liquid jet was measured along the whole jet length. This enabled detailed analysis of the local fluid-dynamics phenomena and to the proposal of a calculation method, based on the classic solution of the thermal field governing equation in the liquid jet [5], for the heat transfer coefficient and jet temperature evaluation. A complete overview of available correlations is also made and comparisons with the experimental data are presented.

2. EXPERIMENTAL APPARATUS

A schematic diagram of the experimental apparatus and of the test section are shown in Fig. 1. The apparatus includes, besides the test section, a water storage tank, an electric heater for water (10 kW), an electric boiler for saturated steam production (15 kW; 20 kg h^{-1}) and an electric heater for steam superheating. The loop characteristics are as follows:

pressure, p	up to 1.0 MPa
water mass flow rate, W	up to 120 kg h^{-1}
steam mass flow rate	up to 20 kg h^{-1}
inlet saturated steam temperature, T_s	up to 160°C
inlet water temperature, T_w	up to 80°C
inlet superheated steam temperature	up to 200°C.

The test section is made up of a cylindrical vessel flanged at the bottom. Steam is introduced from the top of the test section. Water is introduced from the top of the vessel by means of a nozzle. The jet nozzle diameters are 1, 2, 3 and 5 mm, whilst the lengths are 1 and 20 diameters.

The inlet water temperature is measured with a thermocouple just upstream of the nozzle.

The average temperature of the liquid jet is obtained by measuring with a thermocouple the water collected inside a very small pool of Teflon, a sort of 'mixing cup' which can continuously travel along the jet axis. This 'mixing cup' has a very reduced diameter, very close to that of the jet, so as to avoid spoiling the measurement because of condensation on its surface, which can therefore be neglected.

The water mass flow rate is measured by means of turbine flowmeters. The inner diameter of the test section vessel is 160 mm.

3. EXPERIMENTAL RESULTS

3.1. *Test matrix*

Direct contact condensation of saturated steam on a jet of subcooled water has been studied by carrying out 104 tests.

The ranges of the parameters in the experiments are as follows:

saturated steam temperature, T_s	between 105 and 155°C
inlet liquid temperature, T_w	15 and 80°C
liquid mass flow rate, W	between 1.5 and 25 g s^{-1}
inlet mean liquid velocity, u	between 0.08 and 20 m s^{-1}
jet nozzle diameter, D	1, 2, 3 and 5 mm
jet nozzle length, $H/D = H^*$	1 and 20 diameters.

NOMENCLATURE

a, a_1, a_2, a_3	constants
A	parameter defined in equation (39)
A_i	constants in equation (23)
b	constant
B	parameter defined in equation (52)
c_1, c_2	constants
c_p	specific heat
C	parameter defined in equation (53)
D	diameter of the nozzle
F_σ	force due to surface tension
Fr	Froude number
g	gravitational acceleration
h	heat transfer coefficient
H	nozzle length
H^*	dimensionless nozzle length, H/D
k	thermal conductivity
K	Kutateladze number
l	characteristic length
L	jet length
m	constant in equation (53)
Nu	Nusselt number
p	pressure
P	perimeter
Pr	Prandtl number
q''	heat flux
Q	heat transferred
r	radius
R	radius
Re	Reynolds number
S	heat transfer surface
St	Stanton number
t	time
T	temperature
$\Delta T_{\log}$	logarithmic mean temperature difference
u	velocity
W	mass flow rate
We	Weber number
x	coordinate along the jet
X	coordinate, x/D
z	coordinate, $r/R(x)$.

Greek symbols

α	thermal diffusivity
α_i	roots of the first kind, first-order Bessel function
α_L	Laplace constant
β_i	roots of the first kind, zero-order Bessel function
ε	parameter defined in equation (20)
ε^*	parameter defined by Kutateladze, 5×10^{-4}
θ	normalized jet temperature, equation (1)
Θ	normalized jet temperature, equation (18)
λ	latent heat of vaporization
ν	kinematic viscosity
ρ	density
σ	surface tension
τ	time.

Subscripts

f	liquid
G	equivalent
hb	hydraulic break-up
j	jet
max	maximum
n	nozzle
s	vapour
tb	thermal break-up
tot	total
tr	transient
turb	turbulent
x	position of jet temperature measurement device
w	water at nozzle exit conditions
0	nozzle exit conditions
∞	steady-state condition.

The average liquid jet temperature is measured over a length of 250 mm from the nozzle exit; generally, about ten measurements of the jet temperature are performed.

3.2. *Experimental data*

Before presenting the experimental data it is convenient to introduce some variables which will be useful.

Defining x as the distance between the point of jet liquid temperature measurement and the nozzle outlet and T_j the average temperature on the cross-section of the jet at x; we have θ, the jet normalized axial temperature

$$\theta = (T_j - T_w)/(T_s - T_w) \tag{1}$$

h_l, the 'local' heat transfer coefficient

$$h_l = \frac{Wc_p}{P(T_s - T_j)} \frac{\partial T_j}{\partial x} \tag{2}$$

h, the 'average' heat transfer coefficient, between the nozzle outlet and x

$$h = \frac{Wc_p(T_j - T_w)}{S\Delta T_{\log}} \tag{3}$$

where

$$\Delta T_{\log} = (T_j - T_w)/[\ln((T_s - T_w)/(T_s - T_j))] \tag{4}$$

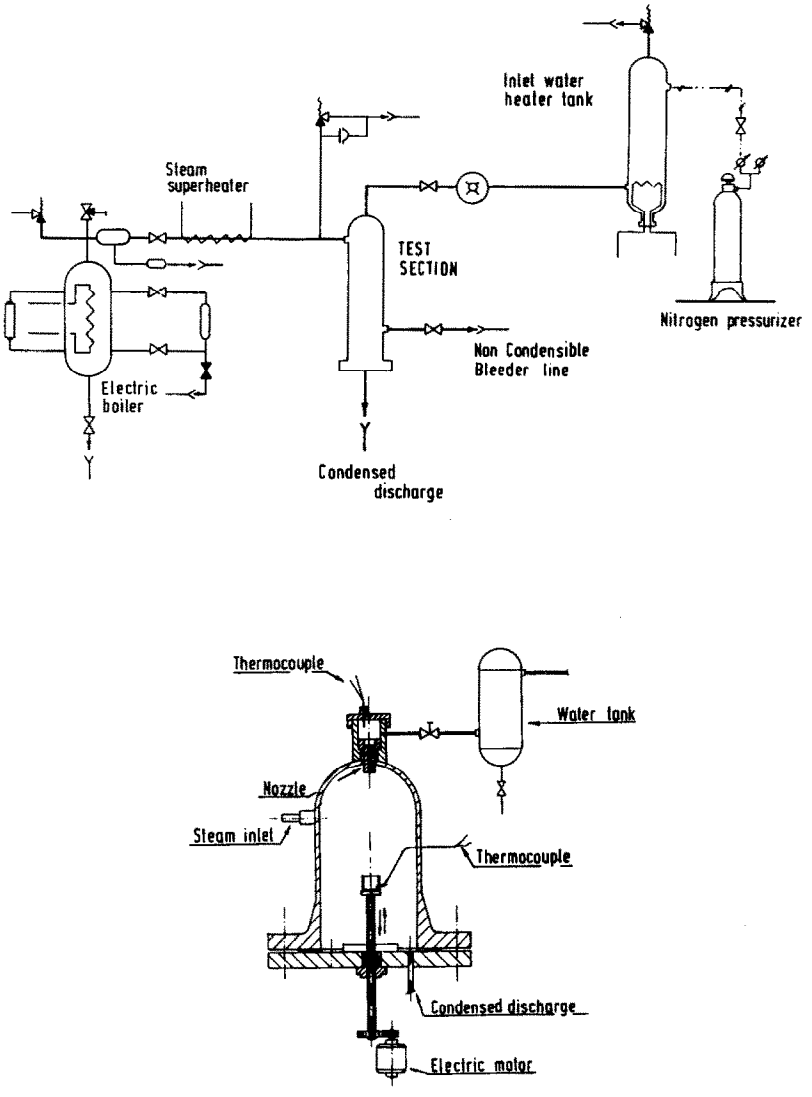

FIG. 1. Schematic of the experimental loop and test section.

P the perimeter of the liquid jet (supposed constant); and S the heat transfer surface between the nozzle outlet and x (i.e. Px).

The Stanton number, St, is introduced as

$$St = Nu/Re\,Pr = h/\rho u c_p.$$

Observing that

$$Q = Wc_p(T_j - T_w) = hS\Delta T_{log} \tag{5}$$

it follows that

$$St = 0.25\frac{D}{x}\ln\frac{T_s - T_w}{T_s - T_j}. \tag{6}$$

Experimental results are reported in ref. [6].

A graphic representation of the experimental data is reported in Fig. 2.

In Fig. 2(a) θ is plotted against the distance from the nozzle outlet, x, for different nozzle diameters and mass flow rates, D and W, with steam and inlet water temperatures, T_s and T_w, as parameters. The normalized jet temperature, θ, turns out to be casually affected by T_s and T_w and, however, within the experimental uncertainty band (discussed in the next section). Such a conclusion was drawn in ref. [7] where direct contact condensation of saturated steam on a horizontal surface of flowing water was investigated.

A similar representation of θ vs x is shown in Fig. 2(b), where the parameter is the inlet water mass flow rate, W. This latter parameter seems to strongly affect the liquid temperature trend along the jet axis.

Considering θ as a reference index for the degree of thermodynamic equilibrium, an increase in W gives rise to an increase of the degree of thermodynamic

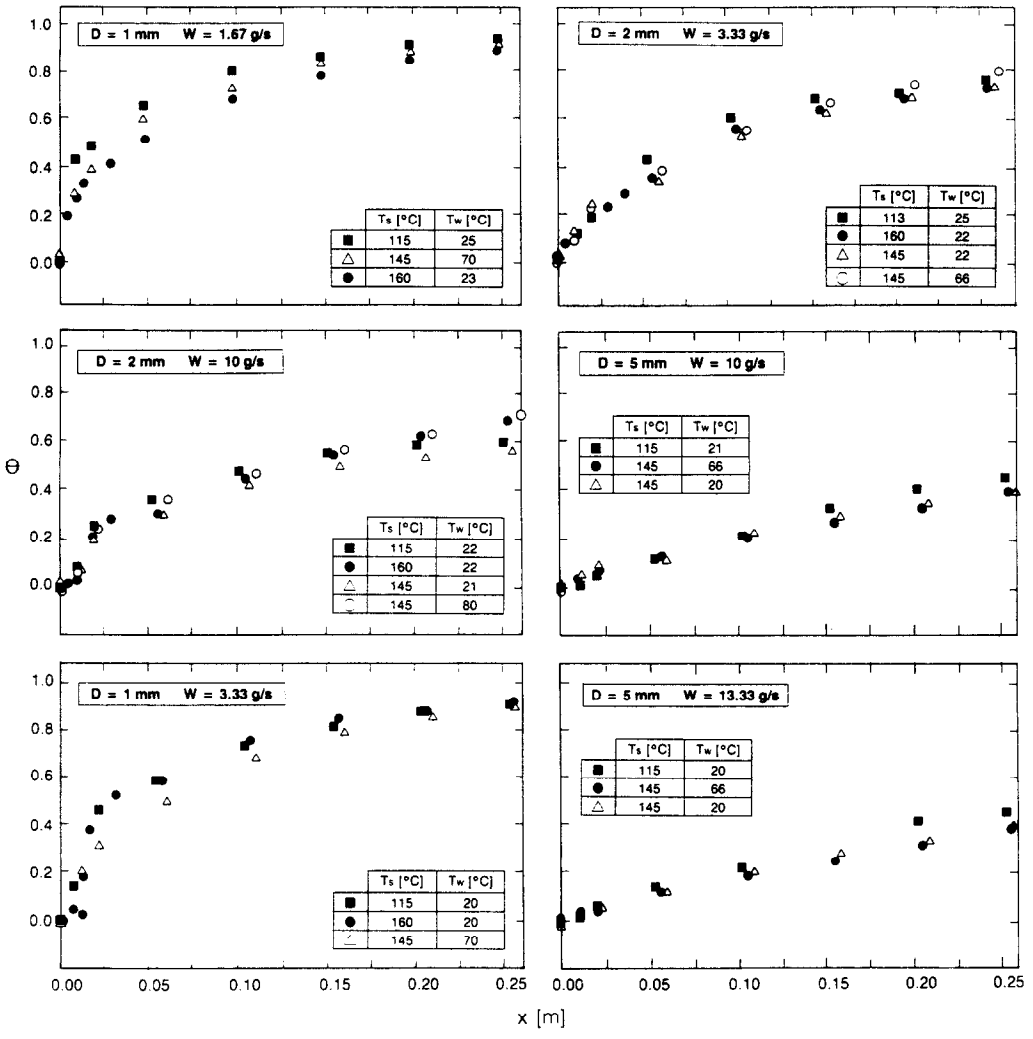

FIG. 2(a). Experimental results: liquid jet normalized temperature vs the distance from the nozzle outlet, with inlet steam and water temperatures as parameters.

equilibrium itself. The effect is enhanced by increasing the nozzle diameter. For the same inlet water mass flow rate, W, we have a higher mean velocity in a jet cross-section with a small nozzle diameter. This produces more significant turbulence effects and hence better heat transfer (i.e. a greater degree of thermal equilibrium).

The influence of the nozzle diameter, D, is evidenced in Fig. 2(c), where θ is plotted against x for two water mass flow rates, with D as a parameter. In Fig. 2(d) the influence of the nozzle length on the trend of θ along the jet axis is shown. Liquid jets from $H/D = 20$ nozzles show a lower heat transfer in comparison with jets from those with $H/D = 1$. In the former nozzles the velocity profile at the exit can be considered completely developed, whilst at the exit of a $H/D = 1$ nozzle the velocity profile is practically flat. The lower peripheric velocity of the developed profile may give way to less heat transfer between the steam and the liquid jet.

As far as the heat transfer coefficient, h, is concerned, the experimental results are plotted in Fig. 2(e). The influence on h of the nozzle diameter and length is shown, as well as the presence of a maximum in the h vs x trend.

3.3. *Error propagation analysis*

An estimation of the maximum error associated with the liquid jet temperature measurement, T_j, has been accomplished. Four different sources of uncertainty have been identified.

(a) The error associated with the evaluation of the distance x from the nozzle outlet at which T_j is measured. It is essentially due to the uncertainty both in the positioning of the movable device and in the water level of the small Teflon pool.

(b) The error associated with the instability of the liquid jet.

(c) The error associated with the steam pressure oscillations inside the test section.

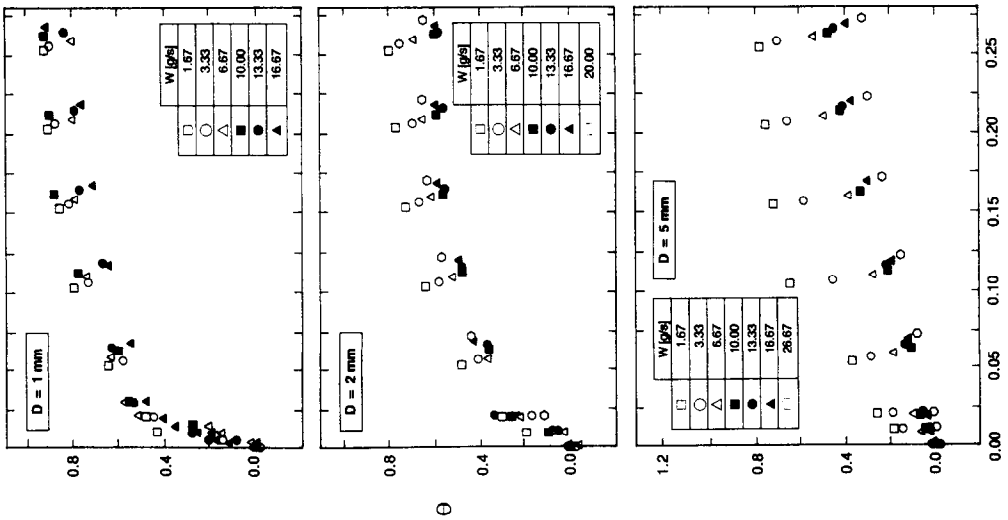

FIG. 2(b). Experimental results: liquid jet normalized temperature vs the distance from the nozzle outlet, with the inlet water mass flow rate as a parameter.

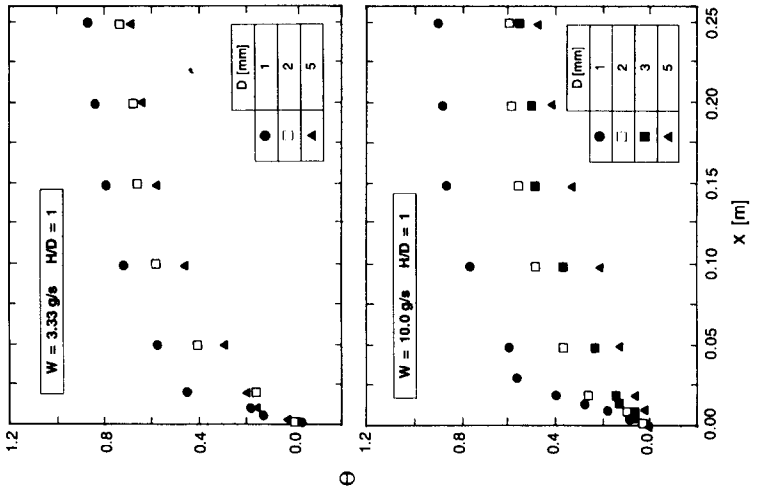

FIG. 2(c). Experimental results: liquid jet normalized temperature vs the distance from the nozzle outlet, with the nozzle diameter as a parameter.

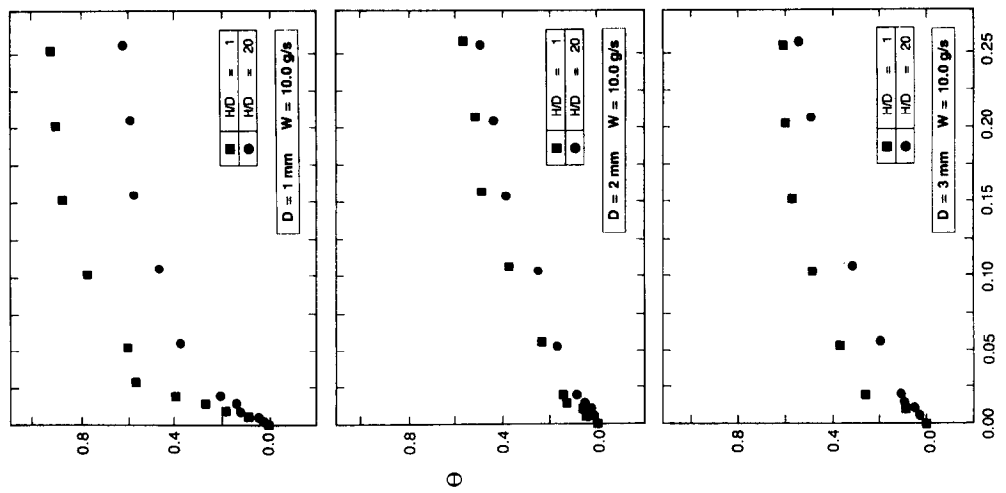

FIG. 2(d). Experimental results: liquid jet normalized temperature vs the distance from the nozzle outlet, with the nozzle length as a parameter.

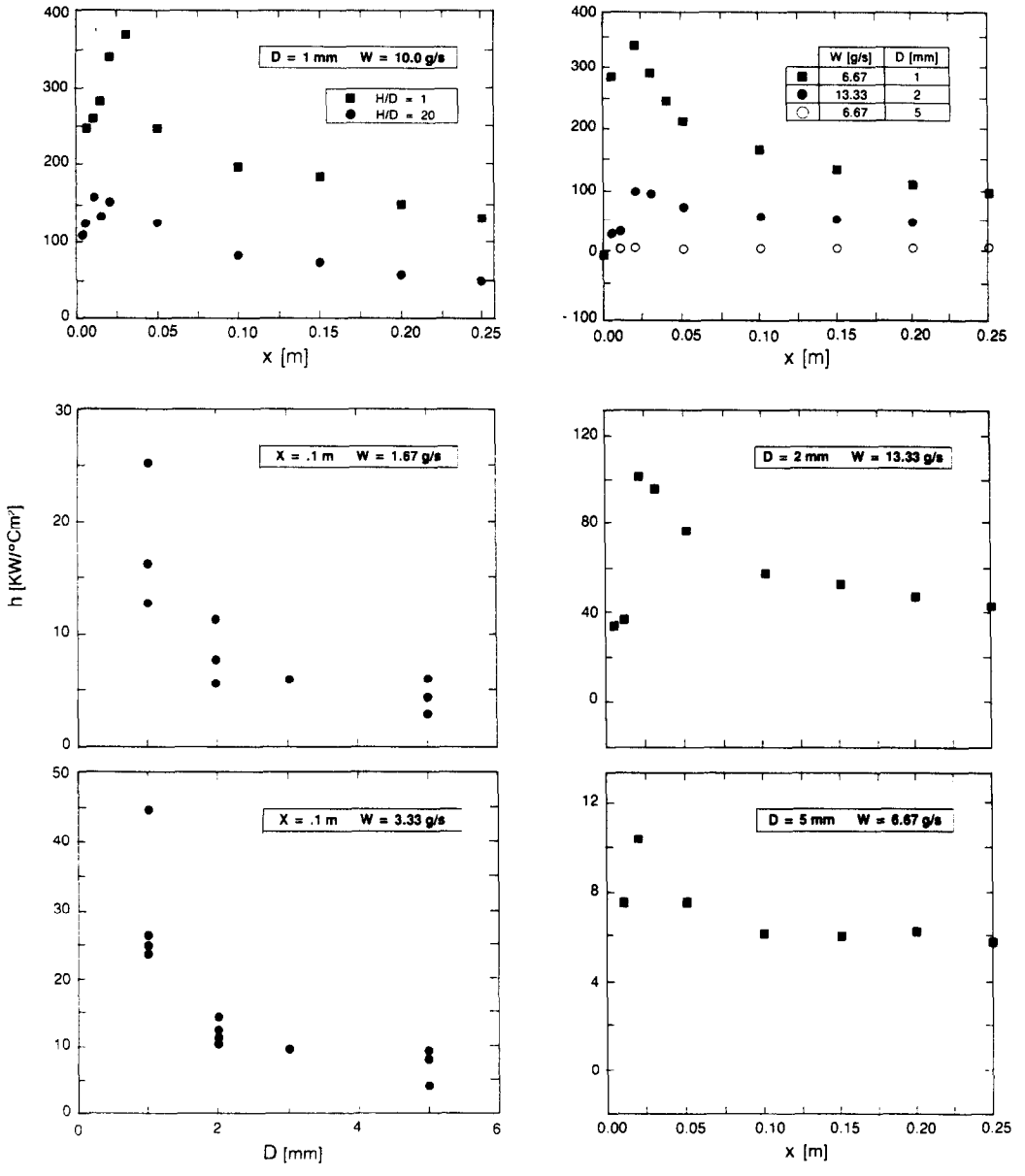

FIG. 2(e). Experimental results: the influence of the nozzle diameter and length, of the water mass flow rate and of the distance from the nozzle outlet on the heat transfer coefficient.

(d) The error associated with the inlet water temperature measurement. Especially in the case of low water mass flow rates, the water was heated by the nozzle walls.

In Fig. 3 the histogram representing the uncertainty for all the data is shown.

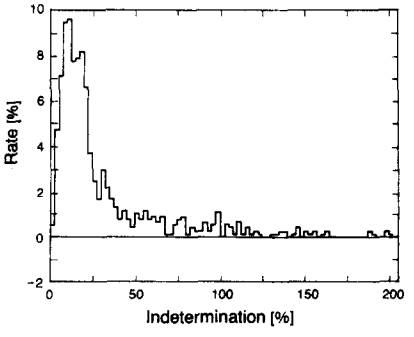

FIG. 3. Spectrum of the experimental uncertainty in the experimental data.

4. COMPARISON OF EXPERIMENTAL DATA WITH AVAILABLE CORRELATIONS

Many correlations are available in the literature to predict the heat transfer coefficient in direct contact

condensation of steam on liquid jets. Such correlations, although effective in describing the heat transfer for the experimental data they refer to, do not generally give an essential contribution to the basic understanding of the phenomenon. Among the tested correlations we selected those proposed by:

Kutateladze [5]

$$Nu = \left(.1 + \frac{\varepsilon^* Du_0}{2\alpha}\right) \frac{\sum_{i=1}^{\infty} \exp\left[-\beta_i^2 f(X)\right]}{\sum_{i=1}^{\infty} \left\{\frac{1}{\beta_i^2} \exp\left[-\beta_i^2 f(X)\right]\right\}} \quad (7)$$

with

$$f(X) = \frac{4\alpha X}{u_0 D^2} + \frac{2\varepsilon^* X}{D};$$

$$\varepsilon^* = 5 \times 10^{-4}; \quad \alpha = \frac{k}{\rho c_p}$$

and β_i the roots of the Bessel function $J_0(\beta_i) = 0$;

Isachenko *et al.* [4]

$$St = 1.2875 \times 10^{-2} (L/D)^{-0.54} \exp(0.135 We_s); \quad (8)$$

Isachenko and Solodov [17]:

if $We_s \geqslant 2.7$

$$St = 0.0335 (L/D)^{-0.42} Re^{-0.17} Pr^{-0.09} K^{0.13} We_s^{0.35} \quad (9)$$

if $We_s \leqslant 2.7$

$$St = 0.03325 (L/D)^{-0.41} Re^{-0.18} Pr^{0.05} \times K^{0.11} \exp(0.16 We_s) \quad (10)$$

with

$$K = \lambda / c_p (T_s - T_w);$$

Benedek [8]

$$St = 0.00286 K^{0.084}; \quad (11)$$

Vasilev (according to Kutateladze) [5]

$$St = 0.01667 (L/D)^{-0.3} Fr^{-0.2}; \quad (12)$$

Sklover and Rodivilin [9]

$$St = 2.7 Re^{-0.4} Pr^{-0.55} K^{0.11} (L/D)^{-0.6} We_s^{0.4}; \quad (13)$$

Iciek [10]

$$St = 0.002675 (L/D)^{-0.27} (We_s Fr)^{-0.7}; \quad (14)$$

De Salve *et al.* [11]

$$St = 3.25 K^{-0.19} Re^{-0.38} Pr^{-0.52} (L/D)^{-0.52}. \quad (15)$$

All the dimensionless groups contained in the above reported correlations, with the exception of the Weber number, We_s, refer to the liquid phase. The liquid physical properties are calculated at the outlet of the nozzle, except for σ, λ and ρ_s which are selected according to saturation temperature. The validity range of the above reported correlations contains the present data.

Amongst the above reported correlations, only the one proposed by Kutateladze [5] is based on a theoretical approach.

Predictions from correlations (7)–(15) are compared with the experimental data in Fig. 4: the agreement is generally poor. In Fig. 5 predictions of the normalized temperature of the jet, θ, vs the jet axis, x, by the correlations of Kutateladze [5] and De Salve *et al.* [11], which revealed to be globally the best ones, are presented.

De Salve *et al.*'s correlation fits the data with an acceptable approximation for situations characterized by a high degree of thermodynamic equilibrium, whilst it gives way to a considerable overestimation of the heat transfer in other conditions. It is evident from Fig. 5 that the overestimation of the heat transfer is in the first part of the liquid jet.

Kutateladze's correlation shows a better 'average' agreement with the experimental data. In fact, because of its theoretical basis, it is able to follow the variations induced by the macroscopic parameters (mass flow rate, abscissa and jet diameter) within the experimetal ranges.

These two correlations, like the other ones tested, do not take into account a parameter which turned out to affect the heat transfer: the length of the nozzle.

As a matter of fact, it is clear that the actual heat transfer behaviour, as a function of the different parameters, is much more complex than the description offered by the correlations tested.

5. DATA ANALYSIS

To be able to represent the phenomenon not only in quantitative terms, but also from a physical viewpoint, it is necessary to develop a local description of the heat transfer between the steam and the liquid jet.

Assuming a flat radial velocity profile in the liquid jet, and constant values of the thermal parameters along the jet axis, and indicating with u_0 the liquid velocity at the nozzle outlet, the thermal balance (neglecting the axial thermal conduction) can be described by means of the following differential equation:

$$u(x) \frac{\partial T_j}{\partial x} = \frac{k}{\rho c_p} \left[\frac{\partial^2 T_j}{\partial r^2} + \frac{1}{r} \frac{\partial T_j}{\partial r}\right] \quad (16)$$

with

$$u(x) = u_0 \sqrt{\left(1 + \frac{2gx}{u_0^2}\right)}.$$

The jet radius along the jet axis, $R(x)$, is given by

$$R(x) = R_0 \sqrt{(u_0/u(x))} \quad (17)$$

where R_0 is the radius of the jet at the nozzle outlet.

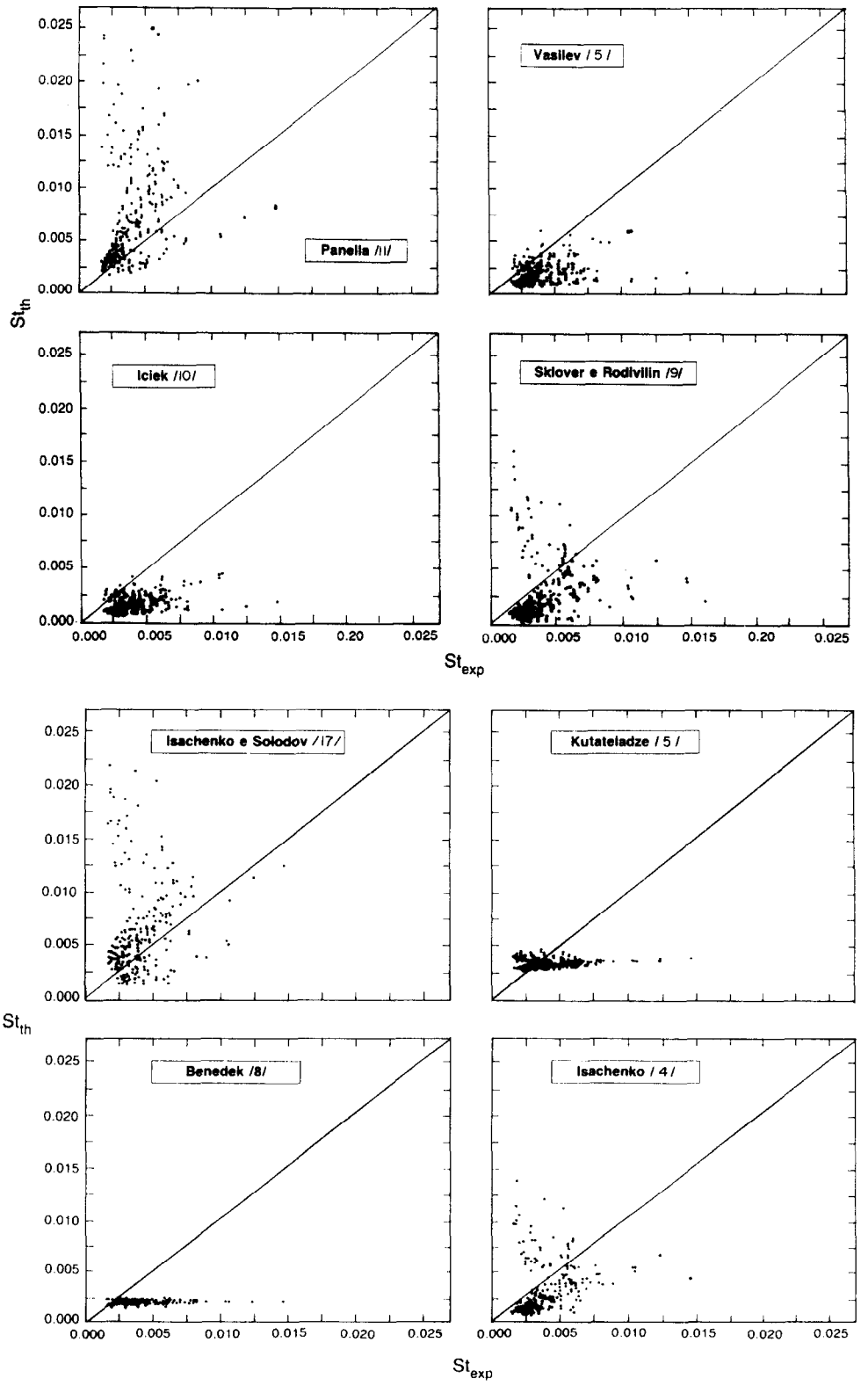

FIG. 4. Comparison of the experimental data with available correlations.

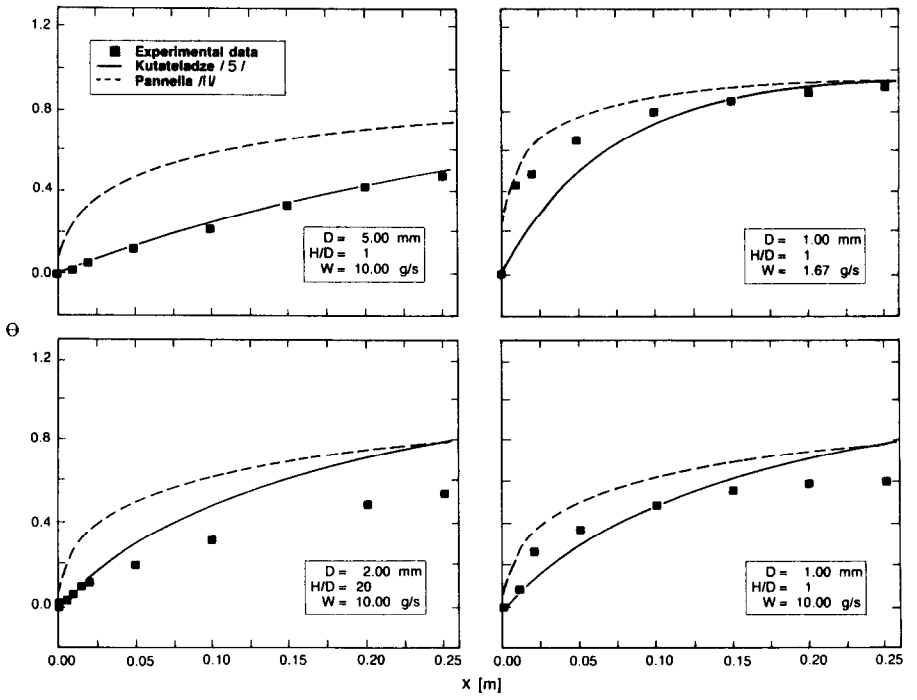

FIG. 5. Local analysis of the experimental data with the correlations of Kutateladze and De Salve *et al.*

Setting

$$X = x/R_0; \quad z = r/R(x); \quad \Theta = (T_s - T_j)/(T_s - T_w) \tag{18}$$

equation (16) becomes

$$\frac{1}{\varepsilon}\frac{\partial \Theta}{\partial X} = \frac{\partial^2 \Theta}{\partial z^2} + \frac{1}{z}\frac{\partial \Theta}{\partial z} \tag{19}$$

with

$$\varepsilon = k/(c_p u_0 R_0 \rho). \tag{20}$$

The general solution of differential equation (19) can be obtained by separating the variables

$$\Theta(X, z) = A\psi(z)\exp[-\beta^2 f(X)] \tag{21}$$

with

$$f(X) = \varepsilon X.$$

Inserting equation (21) into equation (16) gives

$$\frac{d^2\psi(z)}{dz^2} + \frac{1}{z}\frac{d\psi(z)}{dz} + \beta^2\psi(z) = 0 \tag{22}$$

or

$$\frac{d^2\psi(\beta z)}{d(\beta z)^2} + \frac{1}{\beta z}\frac{d\psi(\beta z)}{d(\beta z)} + \beta^2\psi(\beta z) = 0. \tag{22'}$$

Equation (22)—or equation (22')—is known as the Bessel equation, the solution of which is a linear combination of two independent series solutions (cylindrical harmonics) that are called Bessel functions of the first and second kind. Considering the following boundary conditions:

(a) finite temperature of the liquid in the jet axis;

(b) jet surface temperature equal to the steam saturation temperature, i.e. at $z = 1$, $\Theta(X, 1) = 0$ and $\psi(\beta) = 0$;

(c) at the exit of the nozzle, $X = 0$, the liquid temperature has the inlet value, i.e. $\Theta(0, z) = 1$;

the solution is

$$\Theta(X, z) = \sum_{i=1}^{\infty} A_i J_0(\beta_i z)\exp[-\beta_i^2 f(X)] \tag{23}$$

with

$$A_i = -2/[\beta_i J_1(\beta_i)]$$

where J_0 and J_1 are Bessel functions, and β_i's are roots of J_0 [12]. The average temperature along the jet axis is given by

$$\bar{\Theta}(X) = \sum_{i=1}^{\infty}\frac{4}{\beta_i^2}\exp[-\beta_i^2 f(X)] = \frac{T_s - \bar{T}_j(X)}{T_s - T_w}. \tag{24}$$

For what concerns the heat transfer coefficient, h, at a distance x from the nozzle outlet, we have

$$q'' = h[T_s - T_j(x)] = -k\left.\frac{\partial T_j}{\partial r}\right|_{r=R(x)} \tag{25}$$

and then

$$h = -\frac{k}{T_s - T_j(x)} \left.\frac{\partial T_j}{\partial r}\right|_{r=R(x)}. \quad (26)$$

With

$$\left.\frac{\partial T_j}{\partial r}\right|_{r=R(x)} = -\frac{2(T_s - T_w)}{R_0} \times \left(1 + \frac{2gx}{u_0^2}\right)^{1/4} \sum_{i=1}^{\infty} \exp[-\beta_i^2 f(X)] \quad (27)$$

and remembering the definition of Θ, we have

$$h = 2\frac{k}{R_0}\frac{1}{\Theta}\left(1 + \frac{2gx}{u_0^2}\right)^{1/4} \sum_{i=1}^{\infty} \exp[-\beta_i^2 f(X)] \quad (28)$$

and finally

$$h = 2\frac{k}{R_0}\left(1 + \frac{2gx}{u_0^2}\right)^{1/4} \frac{\sum_{i=1}^{\infty} \exp[-\beta_i^2 f(X)]}{\sum_{i=1}^{\infty} \frac{4}{\beta_i^2} \exp[-\beta_i^2 f(X)]}. \quad (29)$$

As can be noted from equations (28) and (29), h assumes an infinite value at the nozzle outlet, $x = 0$ (the jet surface instantaneously reaches the steam temperature) then it quickly decreases to a practically constant value for $f(X) > 0.05$; for high values of $f(X)$ we have

$$\frac{\sum_{i=1}^{\infty} \exp[-\beta_i^2 f(X)]}{\sum_{i=1}^{\infty} \frac{4}{\beta_i^2} \exp[-\beta_i^2 f(X)]} \simeq \frac{\beta_1^2}{4} = 1.446. \quad (30)$$

It is possible to define a heat transfer coefficient at an infinite distance from the nozzle outlet, h_∞, given by

$$h_\infty = \frac{k}{R_0}\left(1 + \frac{2gx}{u_0^2}\right)^{1/4} \frac{\beta_1^2}{2}. \quad (31)$$

The 'transient' (in space terms) expression of the heat transfer coefficient, h_{tr}, can be defined so that

$$h(x) = h_\infty + h_{tr}(x). \quad (32)$$

Mathematically, h_{tr} represents the contribution of the harmonics in equation (29); from a physical viewpoint it represents the settling of the radial temperature profile from a flat shape to a Bessel-type one.

The ratio h/h_∞ can be mathematically approximated by a function of the kind $1 + 1/X$.

As stated by Kutateladze [5] to have an accurate prediction of the phenomenon described by equations (23) and (29) it is necessary to take into account the turbulence contribution in the liquid thermal conductivity, k.

Kutateladze solved the differential equation (16) by adding to the molecular thermal conductivity, k, the contribution given by the turbulence effects, giving way to a total value, $k_{tot} = k + k_{turb}$.

According to Kutateladze

$$k_{turb} = \rho c_p \varepsilon^* R(x) u(x) \quad (33)$$

with

$$\varepsilon^* = 5 \times 10^{-4}.$$

Such an expression for the turbulent thermal conductivity, although enabling the solution of equation (19), does not seem to be exhaustive in describing the local aspect of direct contact condensation of steam on liquid jets, especially for highly turbulent jets, in which k_{turb} as expressed in equation (33), varies slightly along the jet axis (see Fig. 5).

The adoption of a more complicated expression for the total thermal conductivity would make the differential equation (19) very difficult to solve, if not impossible.

Therefore, we solved equation (19) with the hypothesis of a constant thermal conductivity, e.g. the molecular one, and then introduced, as explained in the next paragraph, an equivalent thermal conductivity of the liquid jet, which accounts for all the thermal and fluid-dynamics effects occurring along the jet axis, and not fully described by Kutateladze's approach.

6. A CORRELATION FOR THE INTERPRETATION OF THE EXPERIMENTAL DATA

Celata *et al.* [7] proposed, according to Bird *et al.* [13], the following expression for k_{turb}:

$$k_{turb} = k(a_1 Re^a Pr^a). \quad (34)$$

Such an expression would make equation (19) impossible to solve analytically. Therefore, in the present case we tried a more specific expression of the thermal conductivity to be directly inserted in equation (29).

Turning back to the expression of the heat transfer coefficient, and using equation (31) we can write, with the total thermal conductivity, k_{tot}

$$h(x) = h_\infty + h_{tr}(x) = k_{tot}\left[1 + \frac{h_{tr}(x)}{h_\infty}\right]\frac{\beta_1^2}{2R_0}\left(1 + \frac{2gx}{u_0^2}\right)^{1/4}. \quad (35)$$

To attempt a full description of the turbulent and thermal phenomena along the jet, we define an equivalent thermal conductivity as

$$k_G(x) = k_{tot}[1 + h_{tr}(x)/h_\infty]. \quad (36)$$

All the parameters which significantly affect the heat transfer will have to be taken into account in the calculation of the 'equivalent' thermal conductivity $k_G(x)$.

A correlation of the form given below is proposed

$$k_G(x) = k[1 + A(B(x) + C(x))]. \quad (37)$$

Consequently the heat transfer coefficient can be calculated by

$$h(x) = k_G(x)\frac{\beta_1^2}{2R_0}\left(1+\frac{2gx}{u_0^2}\right)^{1/4}. \quad (38)$$

6.1. *The overall fluid-dynamics effects*

The parameter A in the expression of k_G—equation (37)—takes into account the overall effects of the fluid dynamics of the jet regarding the turbulence of the liquid. The variables supposed to be affecting such a problem are the jet length, H^*, and the Peclet number.

From experimental data

$$A = H^*(Pe)^{(1/H^*)^{0.12}}. \quad (39)$$

6.2. *The local fluid-dynamics effects*

Parameters B and C must take into account the local fluid-dynamics effects, such as the nozzle outlet phenomena and the mechanical interaction between the steam and the liquid, which strongly affect the turbulent thermal conductivity along the jet axis.

From a quantitative viewpoint, the effect of these phenomena has been taken into account by means of a multiplier that modifies the turbulence induced by the nozzle.

The following aspects have been considered:

(a) the effect of the radial velocity profile development along the jet axis;

(b) the decrease of the turbulence because of the lack of solid walls;

(c) the edge effects at the nozzle exit due to the surface tension and to the viscosity;

(d) the effect of the surface instability;

(e) the thermal effect due to the settling of the radial temperature profile;

(f) the effect of the interface shear stress between the steam and the liquid.

Points (a)–(e) are taken into account by B, whilst C refers to point (f).

6.2.1. *The radial velocity profile development.* The liquid inside the nozzle presents a velocity profile determined by the friction with the solid walls. Once the liquid jet is in the steam environment, if we neglect the friction with the gas phase, it tends to assume a flat radial velocity profile.

It would be of interest to evaluate the time requested for the velocity profile adjustment.

The differential equation governing the liquid motion is

$$\frac{\partial u}{\partial t} = \nu\left[\frac{\partial^2 u}{\partial r^2}+\frac{1}{r}\frac{\partial u}{\partial r}\right]. \quad (40)$$

Solving equation (40) for the zone inside the nozzle and for the case of laminar flow (boundary conditions are: (a) velocity at the wall equal to zero; (b) its derivative calculated at $r = 0$ equal to zero) we obtain

$$u(r) = \frac{u_{max}}{R_0^2}(R_0^2 - r^2). \quad (41)$$

At the nozzle exit the boundary conditions are

$$\left.\frac{\partial u}{\partial r}\right|_{r=0} = 0, \quad \left.\frac{\partial u}{\partial r}\right|_{r=R} = 0. \quad (42)$$

In addition, the velocity profile at the outlet must fit the profile inside the nozzle.

As equation (40) is similar to equation (16), it is easy to verify that its solution is given by

$$u(r,t) = \sum_{i=1}^{\infty} A_i J_0\left(\frac{\alpha_i}{R}r\right)\exp\left[-\left(\frac{\alpha_i}{R}\right)^2 \nu t\right] \quad (43)$$

where the α_i's are roots of J_1.

The fundamental harmonic offers an evaluation of the 'adjustment time'

$$\tau = \frac{R^2}{\alpha_1^2 \nu} = \frac{1}{14.67}\frac{R^2}{\nu}. \quad (44)$$

Neglecting the velocity increase along the jet axis, we obtain for the adjustment length

$$\lambda_{a1} = \tau u = \frac{R^2 u}{14.67\nu}. \quad (45)$$

As reported above, in the first part of the liquid jet the external layers are characterized by a velocity lower than the average value: consequently the steam–liquid interaction is attenuated because of the low interface turbulence.

The jet length necessary for the velocity profile adjustment is indicated by λ_{a1} only from a physical viewpoint. Actually this length is much shorter for the following reasons:

(1) the acceleration of the outer layers is essentially due to the harmonics of equation (54), which have time constants lower than the fundamental;

(2) the flow regime inside the nozzle is typically turbulent; therefore, the fluid dynamics of the jet should be studied taking into account the turbulent diffusion of the momentum, practically employing the turbulent viscosity.

For the sake of simplicity, it looks better to define a parameter that could represent this length of superficial turbulence and be correlated to easily measurable macroscopic parameters.

Experiments show a zone of the liquid jet in which the heat transfer coefficient is maximum; we presume that this point is characterized by the highest value of the superficial turbulence.

Such a length, defined as the 'thermal break-up length', may be correlated to the group characterizing λ_{a1} as follows:

$$L_{tb} = 0.75\times 10^{-3}\frac{uR^2}{\nu} + 0.11. \quad (46)$$

It seems reasonable to assume that the interaction between steam and the liquid is maximum when the relative velocity between the two phases is a maximum. The superficial turbulence, then, will undergo an increase of its value along the jet axis, inversely

proportional to the flat velocity profile settling. To take into account this effect we propose

$$B_1 = \exp\left[-\left(\frac{L_{tb}}{x}\right)\left(\frac{H}{D}\right)^{0.3}\right]. \quad (47)$$

The group H/D accounts for the turbulent development inside the nozzle. Correlation (47) shows that for H/D tending to zero, such an effect disappears. Although it is valid for $1 < H/D < 20$, it is reasonable to suppose that for $H/D > 20$, L_{tb} does not vary appreciably.

6.2.2. *Bulk turbulence.* Regarding the above discussed effect, it is necessary to observe that, if the adjustment of the radial velocity profile gives an increase of the superficial turbulence, on the other side it produces a reduction of the bulk turbulence. In fact, with a flat radial velocity profile, the friction among the fluid threads will be reduced.

This effect will be typically asymptotic with a trend similar to that described in Section 6.2.1. The proposed expression is

$$B_2 = \frac{1}{1+a(x/L_{tb})^b}. \quad (48)$$

6.2.3. *Nozzle exit effects.* The external surface of the nozzle exit is wetted by a thin layer of condensed liquid which is connected to the jet liquid. Such a layer is subjected to a holding force towards the nozzle, F_σ, due to the surface tension

$$F_\sigma = \pi D\sigma. \quad (49)$$

This force is a resistance to the slip of the superficial layers, with a reduction of the relative superficial turbulence.

The effect quickly vanishes along the jet axis because of the viscous entrainment. Anyhow it is strongly correlated to the peripherical velocity of the liquid jet and its influence is similar to the effect described in Section 6.2.1. So the term B_3, intended for its mathematical description, can be usefully incorporated in B_1.

6.2.4. *Superficial instability effect.* Superficial instabilities, modifying the shape of the steam–liquid interface, tend to increase the heat transfer. In the studies performed on the superficial instability of jets [14, 15], such disturbances are correlated to the dimensionless group involving mass, viscous and surface tension forces. With the Reynolds number already present in the other terms, experimental tests suggest setting

$$B_4 = \alpha_L/D \quad (50)$$

where α_L is the Laplace constant.

6.2.5. *The radial temperature profile.* As discussed in the first part of this section, the equivalent thermal conductivity has to take into account the quantitative effects of $h_{tr}(x)$. As stated in Section 5, the $h_{tr}(x)/h_\infty$ trend may be approximated with a function such as l/x, where l is a suitable length.

Bearing in mind the expression for B_2, it is useful to approximate both the trends with the following expression:

$$B_2B_5 = \frac{1}{1+a(x/L_{tb})^b}\frac{1}{x} \simeq c_1\left(\frac{L_{tb}}{x}\right)^{C_2}. \quad (51)$$

The term B can be finally given as

$$B = B_1B_2B_3B_4B_5 = 0.00136\left(\frac{L_{tb}}{x}\right)^{1.8}\left(\frac{\alpha_L}{D}\right) \times \exp\left[-\left(\frac{L_{tb}}{x}\right)\left(\frac{H}{D}\right)^{0.3}\right]. \quad (52)$$

6.2.6. *Steam–liquid jet interfacial shear stress.* Independently from the turbulence development of the jet, it is necessary to consider the superficial effect due to the condensed flow rate on the external surface of the liquid jet. It has to be accelerated to the jet velocity.

Practically, one has to add a turbulent term proportional to the condensed mass flow rate. Such a variable is linked, by means of the general heat transfer parameters already present in the other terms mentioned above, to the 'heat transfer driving force'

$$C = m\frac{T_s - T_j}{T_s - T_w}. \quad (53)$$

6.3. *The correlation for the equivalent thermal conductivity, k_G*

In summary, the equivalent thermal conductivity, k_G, can be evaluated by means of the following correlation, where the numerical constants have been obtained by means of a best-fit procedure through the experimental data:

$$k_G = k[1 + A(B+C)] \quad (54)$$

$$A = H^*(Pe)^{(1/H^*)^{0.12}}$$

$$B = 0.00136\left(\frac{L_{tb}}{x}\right)^{1.8}\left(\frac{\alpha_L}{D}\right)\exp\left[-\left(\frac{L_{tb}}{x}\right)\left(\frac{H}{D}\right)^{0.3}\right]$$

$$C = 0.00036\frac{T_s - T_j}{T_s - T_w}.$$

It is now possible to evaluate the heat transfer coefficient using equation (38). The local temperature may be obtained with thermal balances.

The comparison of experimental data with the predictions given by the proposed method is globally shown in Fig. 6 for what concerns the liquid jet temperature, expressed as θ. The agreement is within the experimental uncertainty for most of the data. It is interesting to analyse the goodness of the proposed method in comparison with the correlations of Kutateladze [5] and De Salve *et al.* [11] as in Fig. 7: each point on the curves represents the percentage of data

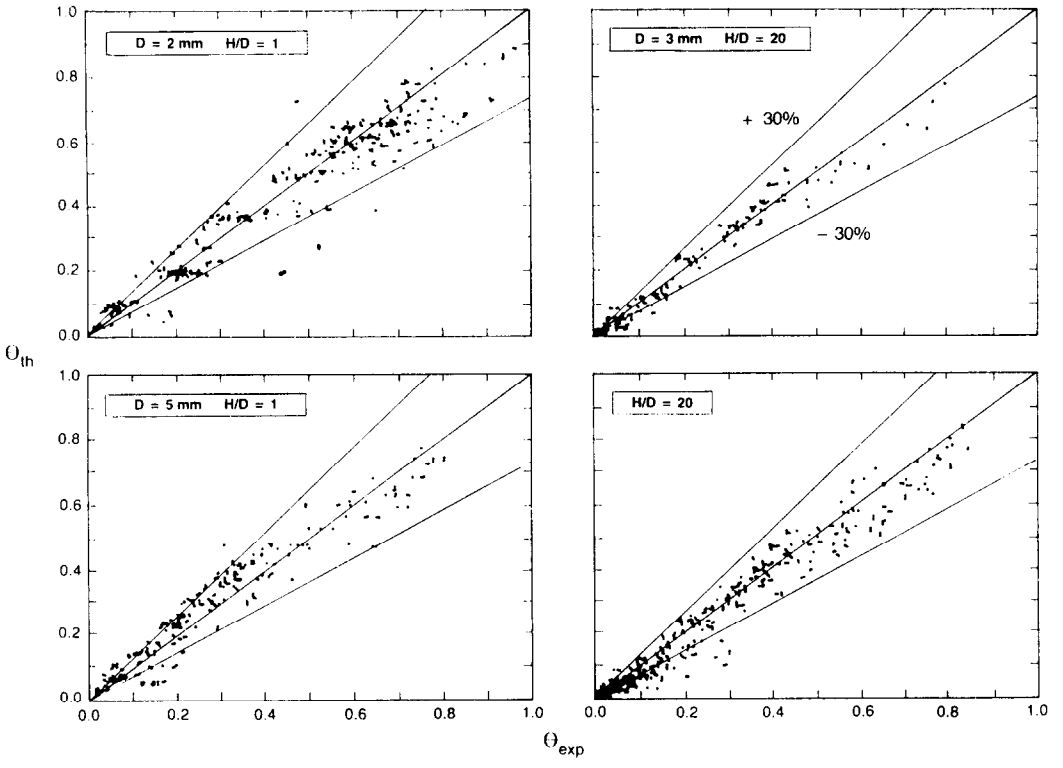

FIG. 6. Comparison between the experimental data and the predictions obtained with the proposed model: the liquid jet normalized temperature.

(ordinate) for which that correlation gives an error greater than the value indicated by the abscissa.

In Fig. 8 typical representations of the liquid jet temperature predictions vs the jet axis are reported.

In these graphs the hydraulic break-up length is plotted (see appendix for its calculation). Beyond this zone the proposed method does not hold any longer; it is interesting to see how its extrapolation enables a good prediction of the phenomenon.

The heat transfer coefficient prediction is represented in Fig. 9 with four typical examples. It must be said that the error propagation strongly affects the estimation of this parameter and above all at a short distance from the nozzle outlet, in which we have a steep variation of $\partial T_j/\partial x$. However, the presence of a maximum and its theoretical prediction is evident.

Figure 10 stresses the influence of H/D on the heat transfer coefficient, h, whilst Fig. 11 shows the influence of H/D on the liquid jet temperature, θ. The proposed method takes into account this interesting experimental evidence very well.

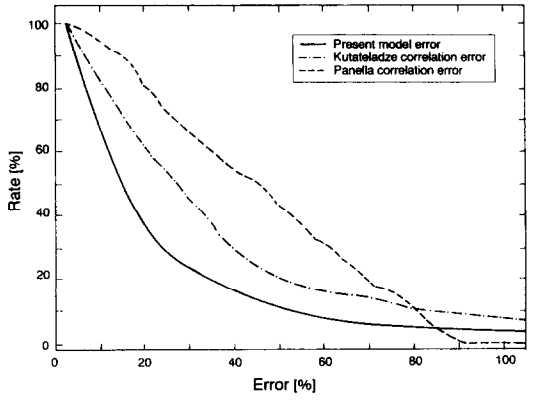

FIG. 7. Comparison among the proposed model performances and those proposed by the correlations of Kutateladze and De Salve *et al.*

7. CONCLUDING REMARKS

Experimental work on direct contact condensation of steam on liquid jets and a thorough analysis of it have been accomplished and presented: the influence of parameters such as steam and water temperatures, water mass flow rate, nozzle diameter and length has been evaluated. Available correlations for the prediction of the heat transfer coefficient, generally empirical, are unable to fully describe the phenomenon.

From the analysis of local and global fluid-dynamics effects, we propose a correlation based on an equivalent thermal conductivity of the liquid jet. Comparison with the experimental data looks acceptable and well within experimental accuracy.

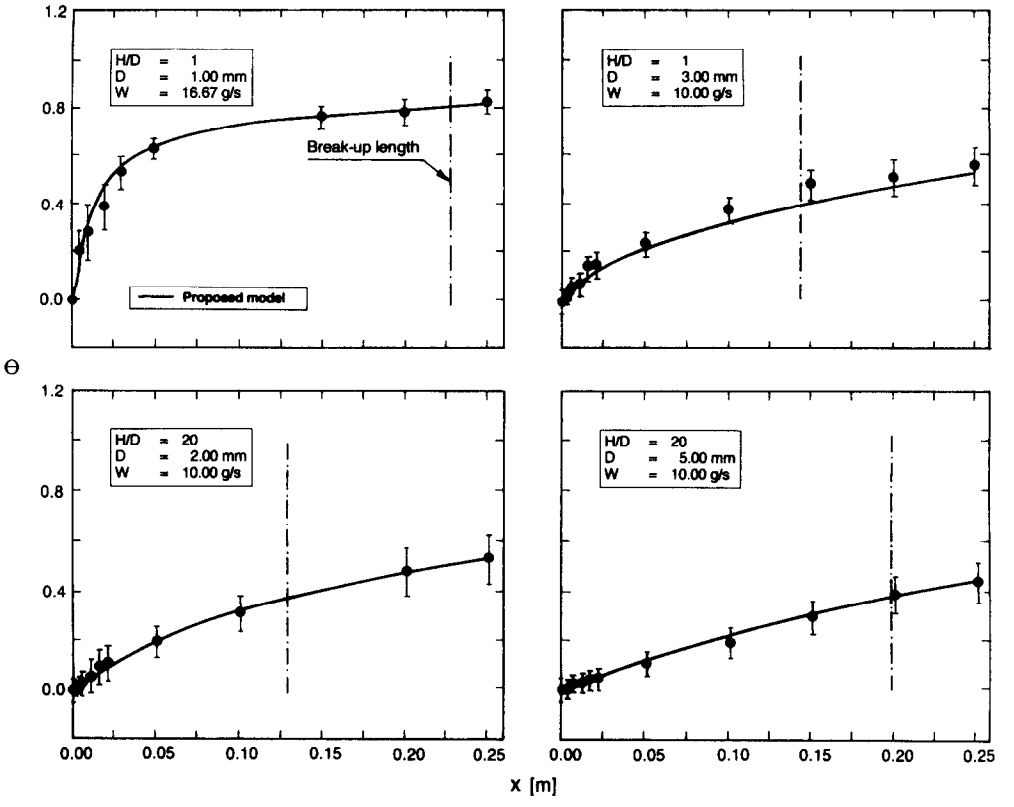

FIG. 8. Typical predictions of the liquid jet normalized temperature with the proposed model.

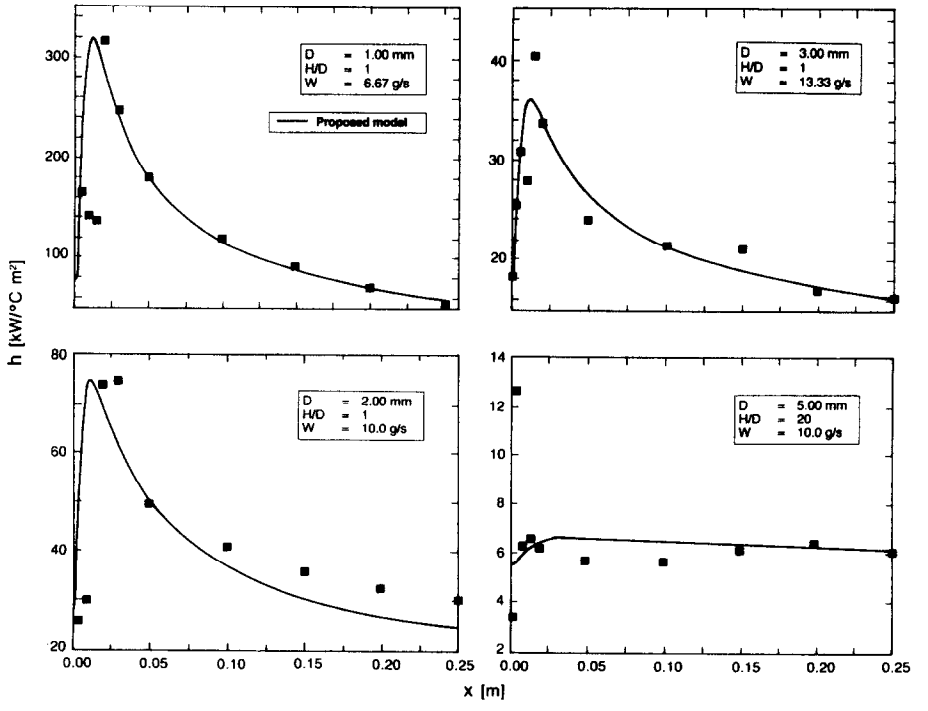

FIG. 9. Typical predictions of the heat transfer coefficient along the jet axis with the proposed model.

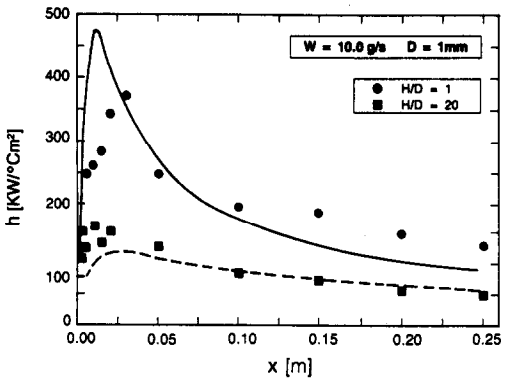

FIG. 10. Prediction of the heat transfer coefficient along the jet axis with the proposed model for short ($H/D = 1$) and long nozzles ($H/D = 20$).

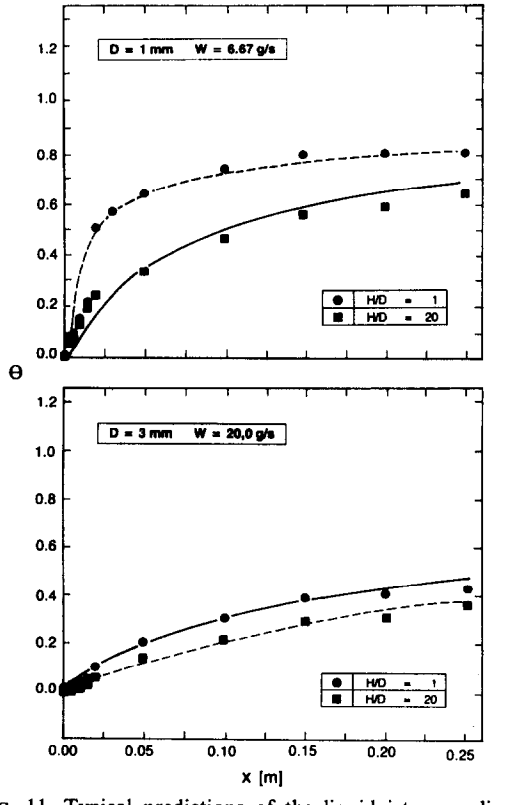

FIG. 11. Typical predictions of the liquid jet normalized temperature with the proposed model for short ($H/D = 1$) and long nozzles ($H/D = 20$).

Acknowledgements—The authors wish to thank Mrs B. Perra for her assistance in editing the paper and Dr F. D'Annibale for the useful discussions during the work.

REFERENCES

1. F. Dobran, Direct contact condensation phenomena in pressurized and boiling water nuclear reactors, Stevens Institute of Technology Technical Report, ME-RT-83004, Hoboken, New Jersey (1983).
2. J. Iciek, U. Cywinska and R. Blaszczyk, Hydrodynamics of free-liquid jets and their influence on heat transfer. In *Handbook of Heat and Mass Transfer*, Vol. 1, pp. 151–181. Gulf, Houston, Texas (1986).
3. M. De Salve, B. Panella and G. Scorta, Fluid-dynamics and heat transfer in direct condensation of steam on a liquid jet, *Proc. 4th Miami Int. Symp. on Multiphase Transport and Particulate Phenomena*, Miami Beach, 15–17 December (1986).
4. V. P. Isachenko, A. P. Solodov, Y. Z. Samoilovich, V. I. Kushinyrev and S. A. Sotskov, Investigation of heat transfer with steam condensation on turbulent liquid jets, *Teploenergetika* **18**(2), 7–10 (1971).
5. S. S. Kutateladze, *Heat Transfer in Condensation and Boiling*, Chap. 7. Moscow/Leningrad (1952), English translation by U.S. Atomic Energy Commission, AEC-tr-3770, 2nd Edn.
6. G. P. Celata, M. Cumo, G. E. Farello and G. Focardi, Direct contact condensation of steam on subcooled liquid jets, Final Report, ENEA RT/TERM 88/1 (1988).
7. G. P. Celata, M. Cumo, G. E. Farello and G. Focardi, Direct contact condensation of steam on slowly moving water, *Nucl. Engng Des.* **96**, 21–31 (1986).
8. S. Benedek, Heat transfer at the condensation of steam on turbulent water jet, *Int. J. Heat Mass Transfer* **19**, 448–450 (1976).
9. G. G. Sklover and M. D. Rodivilin, Heat and mass transfer with condensation of steam on water jets, *Teploenergetika* **22**(11), 65–68 (1975).
10. J. Iciek, The hydrodynamics of a free, liquid jet and their influence on direct contact heat transfer—III. Direct contact heating of a cylindrical free falling liquid jet, *Int. J. Multiphase Flow* **9**, 167–179 (1983).
11. M. De Salve, B. Panella and G. Scorta, Heat and mass transfer by direct condensation of steam on a subcooled turbulent water jet, *Proc. 8th Int. Heat Transfer Conf.*, San Francisco, Vol. 4, pp. 1653–1658, August (1986).
12. W. H. Beyer, *Handbook of Mathematical Sciences*. CRC Press, Boca Raton, Florida (1987).
13. R. B. Bird, W. E. Stewart and E. N. Lightfoot, *Transport Phenomena*. Wiley, New York (1960).
14. R. P. Grant and S. Middleman, Newtonian jet stability, *A.I.Ch.E. Jl* **12**, 669–678 (1966).
15. R. W. Fenn and S. Middleman, Newtonian jet stability: the role of air resistance, *A.I.Ch.E. Jl* **15**, 379–383 (1969).
16. E. Van De Sand and J. M. Smith, Jet break-up and air entrainment by velocity turbulent water jets, *Chem. Engng Sci.* **5**, 32–36 (1976).
17. V. P. Isachenko and A. P. Solodov, Heat transfer with steam condensation on continuous and on dispersed jets of liquid, *Teploenergetika* **19**(9), 24–27 (1972).

APPENDIX

The fluid-dynamics characterization of the nozzle has been based on tests carried out in air and aimed at determining the break-up length [2]. In the field of investigated

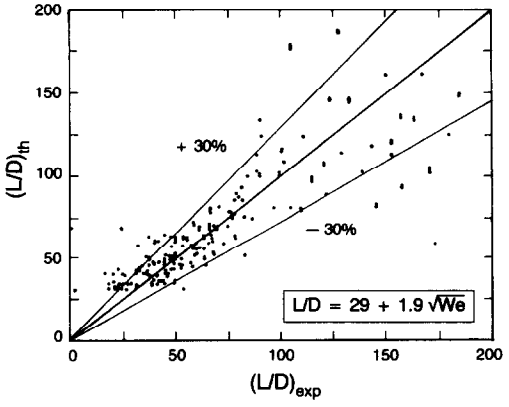

FIG. A1. Prediction of the hydraulic break-up length.

parameters, the jet was characterized by the presence of axial-symmetrical disturbances typical of the condition leading to 'varicose break-up' [16].

The data spread is large and it is due not only to the stochastic nature of the phenomenon but also to the difficulty in adopting a criterion for the definition of the break-up point.

As available correlations cannot predict our data, we propose an empirical correlation to estimate the hydraulic break-up length, L_{hb}

$$L_{hb}/D = 29 + 1.9\sqrt{We}.$$

The relative error turned out to be 22% (Fig. A1).

ANALYSE DE LA CONDENSATION PAR CONTACT DIRECT DE LA VAPEUR D'EAU SATUREE SUR DES JETS LIQUIDES SOUS-REFROIDIS

Résumé—Une expérience sur la condensation par contact direct de la vapeur d'eau saturée sur des jets liquides sous-refroidis, est conduite et appuyée par une analyse théorique des résultats expérimentaux. Des formules disponibles dans la littérature sont généralement incapables de prédire à la fois les conditions locales du jet liquide et le transfert thermique total. A partir de l'analyse des effets locaux et globaux dynamiques, nous proposons une méthode de calcul basée sur une conductivité thermique équivalente du jet liquide. La comparaison avec les données expérimentales semble acceptable parce que dans la précision expérimentale.

EINE UMFASSENDE ANALYSE DER DIREKTKONDENSATION GESÄTTIGTEN DAMPFES AN EINEM UNTERKÜHLTEN FLÜSSIGKEITSSTRAHL

Zusammenfassung—Die Kondensation gesättigten Dampfes bei direktem Kontakt mit einem Strahl unterkühlter Flüssigkeit wird untersucht, die gewonnenen Daten werden theoretisch ausgewertet. Die in der Literatur verfügbaren Korrelationen sind im allgemeinen nicht in der Lage, den lokalen Zustand des Flüssigkeitsstrahls und den Gesamtwärmeübergang zu berechnen. Aufgrund der Analyse der lokalen und globalen Strömungsdynamik schlagen wir eine Berechnungsmethode vor, welche auf einer äquivalenten Wärmeleitfähigkeit des Flüssigkeitsstrahls beruht. Ein Vergleich mit experimentellen Daten zeigt Übereinstimmung im Rahmen der Meßgenauigkeit.

ДЕТАЛЬНЫЙ АНАЛИЗ КОНДЕНСАЦИИ НАСЫЩЕННОГО ПАРА ПРИ НЕПОСРЕДСТВЕННОМ КОНТАКТЕ СО СТРУЯМИ НЕДОГРЕТОЙ ЖИДКОСТИ

Аннотация—Экспериментально исследуется конденсация насыщенного пара при прямом контакте со струями недогретой жидкости, и проводится теоретический анализ экспериментальных данных. Большая часть опубликованных в литературе соотношений не дает возможности определить локальные параметры струи жидкости и суммарный теплоперенос. Предложен метод расчета, в котором использована эквивалентная теплопроводность струи жидкости. Сравнение с экспериментальными данными дает приемлемые результаты и хорошее совпадение в пределах точности экспериментов.